

9/12/90 JSD

CONF 9006.26-1

SLAC-PUB--5305  
DE90 016679

# THE PAD READOUT ELECTRONICS OF THE SLD WARM IRON CALORIMETER\*

P. N. BURROWS, W. BUSZA, S. L. CARTWRIGHT, J. I. FRIEDMAN, S. FUESS, S. GONZÁLEZ, T. HANSL-KOZANECKA, H. W. KENDALL, A. LATH, T. LYONS, L. S. OSBORNE, L. ROSENSON, U. SCHNEEKLOTH,† F. E. TAYLOR, R. VERDIER, B. WADSWORTH, D. C. WILLIAMS, and J. M. YAMARTINO

Massachusetts Institute of Technology, Cambridge, MA 02139, USA

B. L. BYERS, J. ESCALERA, A. GIOUMOUSIS, R. GRAY, D. HORELICK, D. KHARAKH, R. L. MESSNER, J. MOSS, and R. W. ZDARKO

Stanford Linear Accelerator Center, Stanford University, Stanford, CA 94309, USA

Presented by U. SCHNEEKLOTH†

The design of the pad readout electronics of the Warm Iron Calorimeter for the SLD detector at SLAC, consisting of about 9,000 analog channels, is described. Results of various tests performed during the construction, installation and commissioning of the electronics mounted on the detector are presented.

## 1. INTRODUCTION

The SLD detector at SLAC is a general-purpose detector for studying  $e^+e^-$  annihilation at the  $Z^0$  energy range. Its calorimeter system consists of two parts: a lead-liquid argon calorimeter (LAC) and an iron calorimeter (WIC). The LAC has both electromagnetic and hadronic sections, 2.8 absorption lengths in depth, and is located inside the magnetic field coil. The coil is enclosed by an iron/limited streamer tube sandwich calorimeter<sup>1</sup> called the Warm Iron Calorimeter (WIC), which also acts as the flux return for the magnetic field. The limited streamer tubes are read out with strip electrodes for muon tracking and identification and pad electrodes for hadron calorimetry. Most of the energy of hadronic showers is contained in the liquid argon calorimeter, the WIC acting only as a "tail catcher." The energy resolution,  $\sigma_E/E = 80\%/\sqrt{E}$  ( $E$  in GeV) determined with test beam data,<sup>2</sup> is therefore modest compared with the resolution of the LAC of  $55\%/\sqrt{E}$  for hadronic showers.<sup>3</sup>

Pads of different layers of streamer tubes are daisy-chained to form projective towers, pointing to the interaction region, following the geometry of the LAC.

The daisy chains are divided into two sections in depth, which are read out independently. In the barrel the inner and outer octants both consist of 8 pad layers. Similarly, the inner endcaps have 6 and the outer endcaps 8 pad layers. In this paper we will first describe the pad readout electronics and then present the commissioning and test results of the electronics mounted on the detector.

## 2. PAD ELECTRONICS

Data from pad towers are read out through 16 collection points, 8 mounted on the barrel and 4 on each endcap, each comprising a VME crate and the appropriate readout electronics. A schematic diagram of a collection point is shown in figure 1. Pad towers are connected by a 26-conductor (60 conductors in the endcaps) shielded interconnect cable from the daisy chain to a cable card in the back of the VME crate, which plugs into a storage module card in a VME crate. There are four cable card-storage module card sets in the crate. Each storage module card has 72 custom-designed dual channel preamplifier hybrids, resulting in 144 channels per card, and 5 sample and hold devices (CDU's), as shown

\*Work supported by Department of Energy contracts DE-AC03-76SF00515 (SLAC) and DE-AC02-763403069 (MIT).  
† Present address: Deutsches Elektronen Synchrotron and Universität Bonn.

*Invited talk presented at the 2nd International Conference on Advanced Technology and Particle Physics, Como, Italy, June 11-15, 1990.*

MASTER  
cp

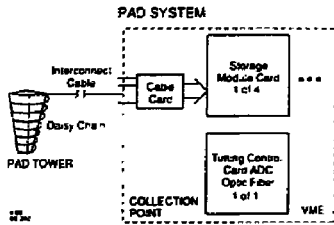


FIGURE 1. Schematic of a collection point.

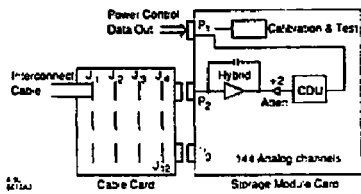


FIGURE 2.

Schematic of a storage module card containing 72 preamplifier hybrids and 5 CDUs.

in figure 2, which are read out serially by the VME controller. The digitized signal is then transformed into optical pulses by a fiber optic auxiliary card and sent to the FASTBUS electronics. After calibration and pedestal subtraction the data are finally sent to the SLD VAX computer. An overview of the system configuration is given in figure 3. In the following section we will give a more detailed description of the essential components of the readout system.

### 2.1. Preamplifier

The preamplifier contains an integrator and a shaping stage. figure 4 shows the schematic of the electrical circuit. Input signals from pad towers are converted to shaped positive-going pulses up to 5.0 V in amplitude, for a maximum input charge of 3.4 nC, which is a factor of two larger than the original design. The output is biased at +0.6 V so that the output signals are in the range +0.6 to +5.6 V. The circuit was designed to have a nominal charge gain of  $1.48 \text{ V/nC} \pm 13\%$ , linear over the full dynamic range. Two measurements are

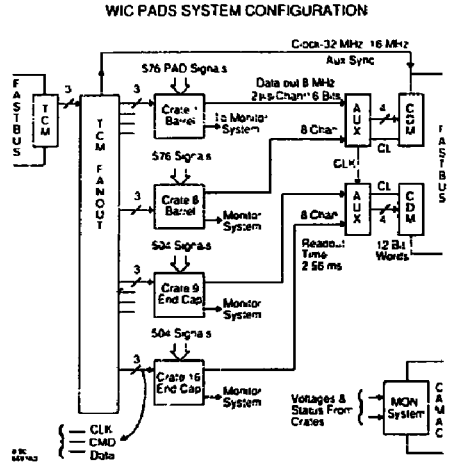


FIGURE 3. Overview of the pad readout electronics.

made on the output: the baseline (pedestal) is measured just prior to the arrival of the signal, the output signal is measured at its peak approximately  $6 \mu\text{s}$  after the beam crossing. The preamplifier is protected against breakdown or discharges in the streamer tubes, which can result in abnormally large signals in a pad tower, by internal diodes connected to +8 V and  $-1.2 \text{ V}$ , respectively.

The circuit design provides several features for internal calibration of the gain, capacitance measurements and continuity checks, which are useful for the debugging and operation of the readout system. The charge gain of the preamplifier can be checked by discharging a precision capacitor ( $680 \text{ pF} \pm 1\%$ ) into the input ( $V_{cal}$  option). It is charged by applying a positive-going voltage step of up to 5 V amplitude with 300 ns rise time. If a channel is selected for calibration,  $V_{cal}$  injects a known charge into the preamplifier and the gain is determined by measuring the voltage on the output.

The capacitance of a pad tower can be measured by applying a negative voltage,  $V_{test}$ , of magnitude 0 to 5 V with 300 ns rise time, to the noninverting input of the operational amplifier. This provides a continuity check from the cable card through the interconnect cable to

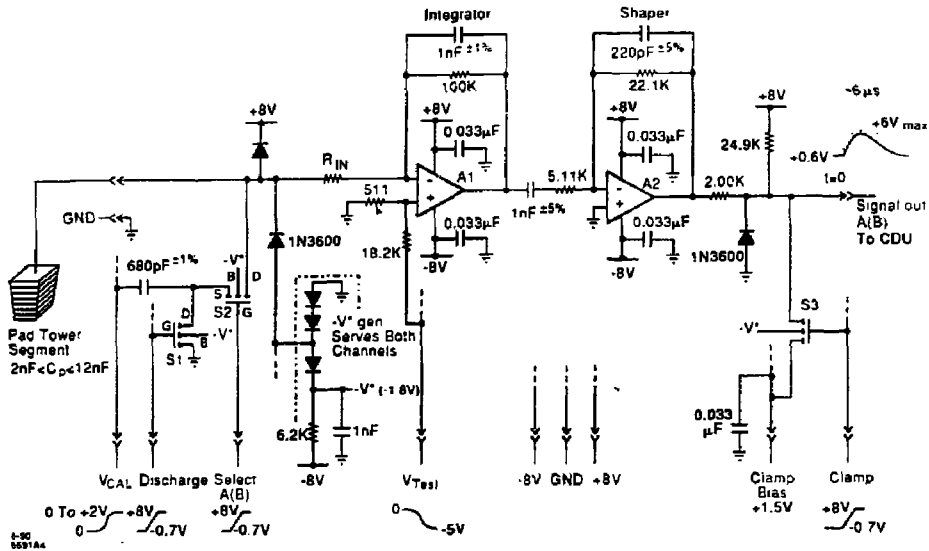


FIGURE 4.  
Schematic of the preamplifier hybrid.

the daisy chain and indicates whether all pads forming a tower are properly connected. The output signal of the preamplifier is a function of the input voltage ( $V_{test}$ ) and of the total source capacitance ( $C_{pad}$ ) connected to the input:  $V_0 = -0.041 V_{test} (1 + C_{pad}/C_F)$ , where  $C_F$  is the feedback capacitor,  $C_F = 1 \text{ nF} \pm 1\%$ . The pad tower capacitances vary between a few and 20 nF in the barrel, 15 nF being typical; the variation is much larger in the endcaps, the highest value being 50 nF.

The clamp option sets the output of the preamplifier to a clamp bias of +1.5 V. This is used for testing purposes of the sample and hold readout electronics.

The preamplifier was built as a dual-channel 15-pin hybrid, manufactured by Tong Hsing Electronic Industries in Taiwan.<sup>4</sup> There are 9,216 channels in the system, including some channels in the endcaps which are not connected to towers, which require 4,608 hybrids. The total number of operational pad towers is 8,640.

Figure 5 shows the charge gain of a typical hybrid, measured using the  $V_{cal}$  mode, compared with a straight line fit to the data. The gain is linear up to around 3.4 nC, which is about twice the original design

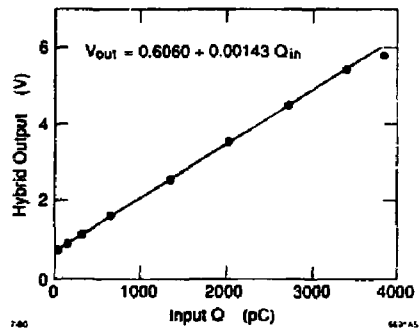


FIGURE 5.

Gain of preamplifier hybrid; output voltage as a function of the input charge.

specification. In fact, the gain of the preamplifier was reduced by a factor of 0.543 by an external 2.2 k $\Omega$  resistor connecting ground with the output of the hybrid, as shown in figure 2. This modification was implemented after it had been decided to operate the streamer tubes with a nonflammable gas mixture, which increased the original estimated gas gain by about a factor of two.

The attenuation also gives a better match to the input characteristics of the sample and hold unit (CDU). The signal levels and gain values given in this paragraph are for hybrids without the external attenuation resistor, but all results presented in the following are for the final configuration with the reduced gain.

### 2.2. Calorimeter data unit

The output of a hybrid is fed into a multichannel sample and hold device, the calorimeter data unit (CDU), a modified version of the circuit developed for the readout electronics of the liquid argon calorimeter.<sup>5</sup> Each calorimeter data unit provides 32 parallel inputs for analog signals and the capability of sampling at two different times. The first sample is used for pedestal measurements and the second for the signals, which are sampled at the peak about 6  $\mu$ s after the beam crossing. Figure 6 shows the linearity of a CDU channel; it starts to saturate at an input voltage of about 3.0 V.

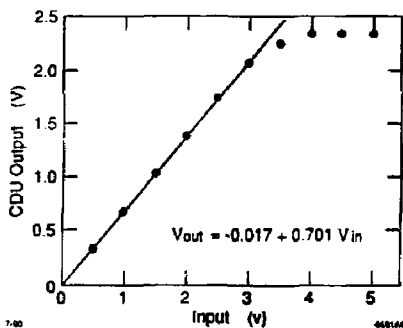


FIGURE 6.

Gain of a CDU channel; output voltage as a function of the input voltage.

### 2.3. VME controller

The VME controller generates the timing and control signals to store data in the calorimeter data units on the storage module cards when it receives timing signals from the FASTBUS Timing and Control Module (TCM). Data from the CDUs are read out serially, digitized by a 12-bit ADC and then sent to the FASTBUS

TABLE 1.  
VME controller commands.

Command	Name	Comment
1	Select crate	Applies to commands 2-5
2	Load $V_{cal}$ DAC	Calibration
3	Load $V_{test}$ DAC	Capacitance measurements
4	Load cal patt	Calibration pattern
5	Reset cal	Reset calibration pattern
6	Run cal reverse	Calibrate pedestal channels
7	Run cal normal	Calibrate signal channels
8	Run normal	Data taking ( $e^+e^-$ or cosmic)
9	Run $V_{test}$	Capacitance measurements
10	Run data test	Set all data bits 1
11	Run clamp test	Set hybrid output to clamp bias

electronics as 16-bit words, including framing and parity bits. The readout time is 2.56 ms for one crate at a bit transfer rate of 8 MHz. There are 1280 words of 16 bits. Data and control signals to the storage module cards are transmitted through the backplane of the crate, which is also used for power distribution. Readout and communication with the FASTBUS electronics is passed through the fiber optic auxiliary card, inserted into the back of the crate. There are four optical fibers for each crate: command, clock and data lines from the FASTBUS TCM, and the serial data out line connected to the FASTBUS CDM.

A summary of the various control commands for readout, calibration and system diagnostics is given in table 1. Commands 1-5, addressed to individual crates, are commands used for selecting a VME crate, the loading of DAC values for calibration or capacitance measurements and for the resetting of calibration patterns. Commands 6-11 are global system running commands, applying to all 16 crates regardless of whether they have been selected. The *Run Cal Reverse Timing* and *Run Cal Normal Timing* commands run a complete calibration cycle to all crates with the calibration pulse timed to occur at the baseline sample (command 6) or with normal timing (command 7) to calibrate the pedestal and signal gains independently. Command 8 (*Run Normal*) executes a normal physics data taking sequence.

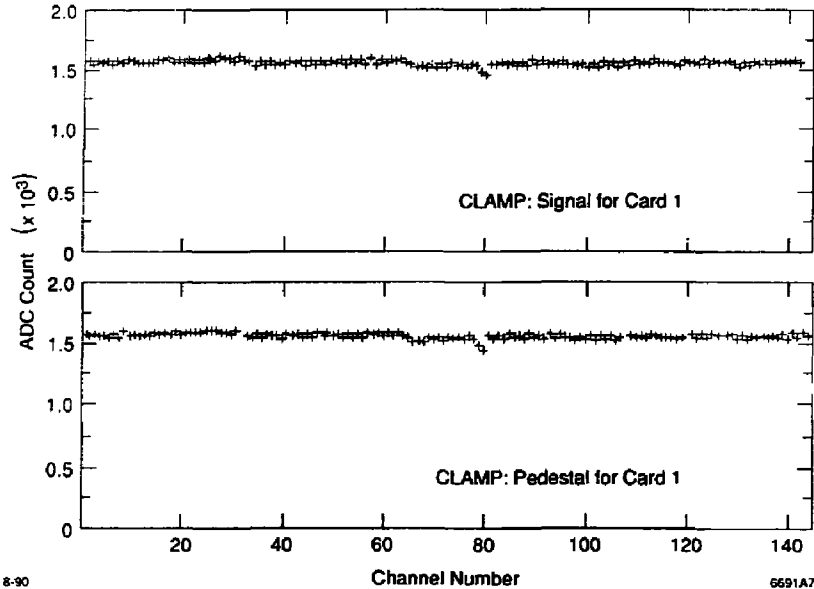


FIGURE 7.  
Clamp test on the detector; ADC counts as a function of channel number.

which is also used for cosmic ray running although with different timing from the FASTBUS TCM. A complete  $V_{reset}$  cycle is performed if command 9 is issued. The *Run Data Test* command (command 10) runs a data acquisition cycle with all bits set to one, used for system diagnostics and for adjustment of the overall system timing. Finally, command 11 runs a data taking cycle with the output of all preamplifiers set to the clamp bias of about +1.5 V; this is used for diagnostic purposes.

#### 2.4. FASTBUS electronics

The FASTBUS electronics consists of a Timing and Control Module (TCM),<sup>6</sup> which drives the VME controllers, and two Calorimeter Data Modules (CDM),<sup>7</sup> one for the barrel and one for both endcaps, each with an auxiliary card<sup>8</sup> for buffering the data. Each CDM has four channels, each having one Digital Correction Unit (DCU),<sup>9</sup> which does the pedestal subtraction and corrects for nonlinearities of the gain by performing a 16 piecewise linear interpolation. The system

configuration is summarized in figure 3. Details about the FASTBUS components can be found in the corresponding references.

### 3. COMMISSIONING AND TEST RESULTS

After production, all components of the readout electronics were extensively bench-tested in the laboratory. Readout cables were tested by hand. A CAMAC-based system was developed for commissioning, using a CAMAC version of the TCM and auxiliary card with the capability of reading out one collection point. The CAMAC TCM, which requires a prebeam signal for triggering, was triggered by a pulse generator. All production units were checked out using this setup before they were installed in the various collection points. Each collection point was then read out in turn. In addition the capacitance of all pad towers connected to the readout cables was measured by hand. All problems such as shorted pads or bad connections were repaired, except for a few pads (at the  $10^{-4}$  level) that were

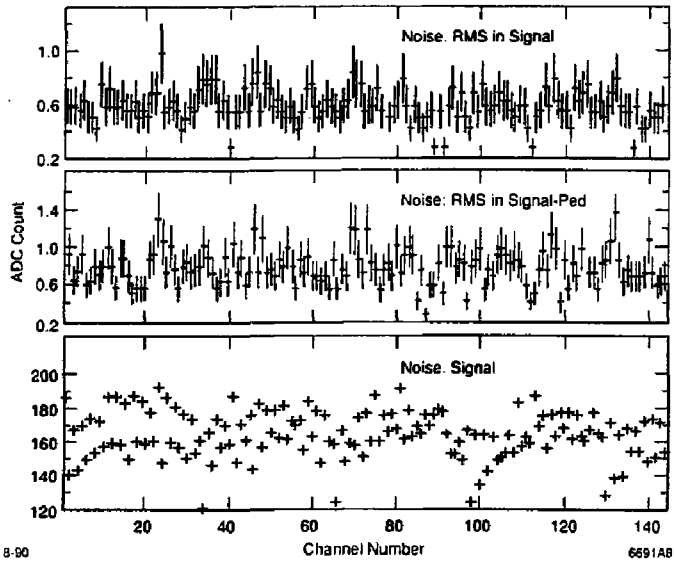


FIGURE 8.

Noise measurement on the detector; ADC counts as a function of channel number.

unrepairable and had to be disconnected from the daisy chain. Finally, the commissioning setup was converted to the final FASTBUS electronics for reading out the entire detector and for cosmic ray data taking. The following section describes the results obtained during the commissioning. All ADC values represent the average of ten independent samplings, with the r.m.s. deviation shown as the error bars.

### 3.1. Data test ( $D_{test}$ )

The timing of the "aux sync" signal from the TCM to the auxiliary card, which indicates the arrival of the first data word from the VME controller, was adjusted using the  $D_{test}$  command, i.e., the 12 data bits in the data field of every data word were set to one.

### 3.2. Clamp test

The results of the clamp test are shown in figure 7, where the ADC value is plotted as a function of the channel number. The outputs of all channels are centered around 1600 ADC counts, with a r.m.s. variation

between cards of 8%. This is as expected for a clamp bias on the output of the hybrid of  $1.5 \text{ V} \pm 10\%$  and ensures proper connections of the various components and also checks the gain of the CDU.

### 3.3. Noise test

The noise level of the readout electronics was measured by running the data acquisition cycle with a VME crate in the laboratory and also with a crate fully connected to the detector, but with the high voltage and the strip readout electronics of the limited streamer tubes not turned on. In both cases the noise level was found to be small and practically undetectable. Figure 8 shows the noise for all channels of a storage module card connected to the detector. The r.m.s. of the difference between signal and pedestal samples is typically less than 1 count, indicating that the noise level is small. Subsequent noise measurements, taken with the high voltage on and the strips readout running, have shown that the noise level is only very slightly higher, and is generally less than 3 ADC counts.

### 3.4. Capacitance measurements ( $V_{test}$ )

The result of the capacitance measurements using the  $V_{test}$  option is shown in figure 9, where the output voltage, in ADC counts, is plotted versus the channel number. Clearly visible is a periodic structure, which corresponds to the geometry of the pad towers. Towers are read out in rows of constant azimuthal angle, starting at the center of the detector. The area of pads forming towers increases towards the end of the barrel, resulting in proportionally increasing capacitances and therefore  $V_{test}$  outputs. The tower capacitance drops off at the end of the barrel, because the tower continues in the endcap, which is read out by a different collection point. The  $V_{test}$  feature is particularly useful for finding shorted or disconnected pads, which are indicated by abnormally high or low capacitance values. In figure 9 the high reading of channel 42 is an example of a tower shorted to ground.

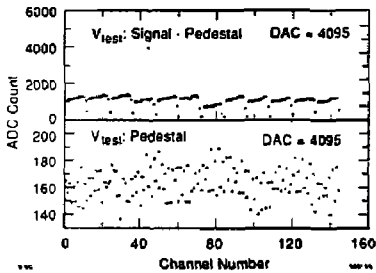


FIGURE 9.

Capacitance ( $V_{test}$ ) measurements; ADC counts as a function of channel number.

### 3.5. Calibration ( $V_{cal}$ )

The combined gain of the preamplifier and CDU was calibrated using the  $V_{cal}$  option. Charge values from 0 to 3.4 nC were injected into each hybrid, separately for signal and pedestal channels, and a linear fit was performed to the measured ADC counts as a function of the DAC value. The gain distribution of all channels of a typical storage module card is shown in figure 10. The mean value of the gain is  $0.85 \pm 0.02$  ADC counts/DAC, corresponding to 1.02 ADC counts/pC. In addition to

gain variations of the electronic components, the gain depends slightly upon the tower capacitance: it is reduced for large capacitances due to the longer integration time of the hybrid. This effect is inherently corrected by the calibration. The calibration of the final system will be performed by the DCU using a piecewise linear interpolation for both signal and pedestal channels.

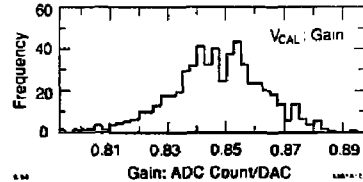


FIGURE 10.

Histogram of the combined gain of preamplifier hybrid and CDU.

### 3.6. Cross-talk measurements

The electronic cross-talk of neighboring channels was studied using the calibration feature of the hybrids, pulsing even-numbered channels and measuring the signals induced in odd-numbered channels and vice versa. The resulting cross-talk is less than 1%, significantly less than the physical cross-talk, which can be as high as 10% as determined by test measurements.<sup>10</sup>

### 3.7. Cosmic-ray data taking

Cosmic ray data were taken using the strip readout electronics to provide a trigger for the FASTBUS TCM. Hits in chambers of opposite octants were required to select tracks of approximately  $90^\circ$  of incidence with respect to the octant read out by the pad electronics. A cosmic ray event is shown in figure 11, where the collected charge in the inner and outer octant is displayed as a function of the  $\theta$  and  $\phi$  position of the pad tower. The distribution of the pulse height is given in figure 12. The pulse height was corrected for variations in the gain of the electronics, using the calibration procedure described in section 3.5. Pedestals were subtracted from the corresponding signal channels. The charge was,

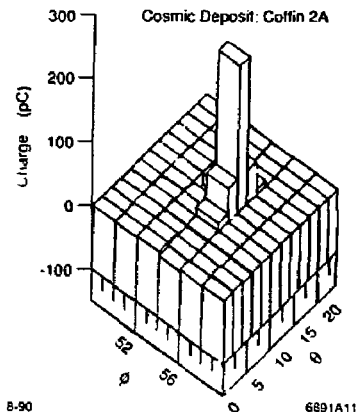


FIGURE 11.

Display of a cosmic ray event in a quadrant of the inner octant. The collected charge is displayed as a function of the  $\theta$  and  $\phi$  position of the pad tower.

however, not corrected for geometric effects, such as the angle of incidence and the number of pads of a tower traversed by the track. The calorimeter, including the readout electronics, behaves as expected with a very low noise level. Systematic studies of the performance are in progress.

#### 4. CONCLUSIONS

The components of the pad readout electronics have been manufactured and mounted on the detector. The complete detector can be read out with the final FASTBUS data acquisition system. Cosmic ray data are taken routinely, indicating that the system behaves as expected. Further software development for calibration and data acquisition is in progress.

#### ACKNOWLEDGMENTS

We would like to thank R. Parsons, N. Ericson, R. Seefred, B. Baer, and C. Schmeizl for their contributions to the construction and testing of the electronics. The contributions of L. Paffrath, J. Fox, G. Haller, and M. Breidenbach are gratefully acknowledged. One of

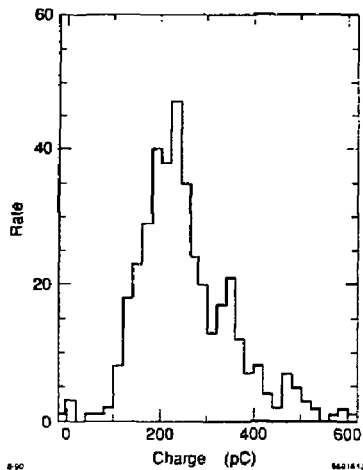


FIGURE 12.

Cosmic ray pulse height spectrum, corrected for gain and pedestal subtracted, but without corrections for the angle of incidence.

the authors (U.S.) would like to thank the DESY directorate for providing the travel funds for attending the conference.

#### REFERENCES

1. A. C. Benvenuti *et al.*, Nucl. Instr. Meth. A276 (1989) 94.
2. G. Callegari *et al.*, Nucl. Sci. Symp. 201 (1985).
3. R. Dubois *et al.*, Nucl. Sci. Symp. 194 (1985).
4. Tong Hsing Electronic Industries, Ltd., Head Office: 4F 85 Yenping Road South, Taipei, Taiwan.
5. G. M. Haller *et al.*, IEEE Trans. on Nucl. Sci. 33 (1986) 221.
6. FASTBUS TCM, SLAC internal communications.
7. FASTBUS CDM, SLAC internal communications.
8. FASTBUS Auxiliary Card, SLAC internal communications.
9. S. Mac Kenzie *et al.*, Nucl. Sci. Symp. 250 (1986).
10. A. C. Benvenuti *et al.*, Nucl. Instr. Meth. A290 (1990) 353.